Velocity Independent Extrapolation Off Wide Offsets of Gathers

Rick Ottolini

This paper presents two schemes for extrapolating missing data at wide offsets off gathers. One scheme is a migration-diffraction to time-depth coordinates. The other is a gather deformation into offset-squared time-squared coordinates. Missing wide offsets is the bane of slant stacking (Schultz SEP-8) and multiple elimination (Thorson, this SEP volume). Velocity independent schemes are desirable in the situations where (1) velocity is not well known, (2) there are both multiples and primaries, and (3) there are both flat and dipping events.

Previous Methods

Previous extrapolation methods include:

(1) Migration-diffraction. One migrates a gather and diffracts the zero offset trace. Ottolini (SEP-25) showed that missing data artifacts don't affect the zero offset trace.

(2) Auto-regressive prediction. (Thorson, this SEP volume) One Fourier transforms the time axis of the dataset in order to make it appear more laterally stationary. Then each constant frequency strip is extrapolated using the Burg algorithm. This method works best on linear segments in the data, so the data is pre-deformed by normal moveout.

(3) Dip prediction. Dips are measured from the widest offsets by cross-correlation. Events on the widest offset trace are extrapolated at these dips.

Some problems with these methods are due to the fact that they are not velocity independent. Problems include:

(1) One needs to know the velocity to migrate, or apply normal moveout.

(2) Adding variable velocity to the above extrapolation algorithms makes them more complicated.

(3) Some datasets have multi-velocity events adjacent to each other such as primaries

and multiples or two different dips. The above extrapolation methods must select one of the velocities.

New Methods

The two schemes presented in this paper are discussed in the context of Claerbout's data restoration framework (SEP-25). That is, data space is first transformed into a model space where events are more parsimonious. Then in model space, events are made to look like what they would have appeared had the data space been better sampled.

The first scheme, the time-depth transformation, is the set of zero offset traces extracted from a gather which has been downward continued to various depths. A version of this transformation has been used by Doherty (SEP-1), Gonzalez (SEP-16), and Yilmaz (1980 SEG). A quick, reversible implementation is formulated as a Stolt algorithm. The parsimony of time-depth space is that hyperbolic events are migrated to some sort of focus with the quality of the focus depending upon the distribution of data offsets and transformation velocity (see figure 2).

The second scheme is a more robust pre-deformation of the gather than normal moveout for the auto-regressive prediction method. This is the offset-squared time-squared resampling of the data first suggested by Cecil Green in an early volume of Geophysics. The parsimony of this model space is that hyperbolic events map into lines (see figure 12). The slope of the line depends upon the velocity of the hyperbola.

A Stolt Formulation of the Time-Depth Transform

The time-depth ($t - \tau$) coordinate transformation is similar to wave equation stacking. Both start with the CMP gather at (h,t,τ=0), then extrapolate (h,t,τ) using the wave equation. However, the $t - \tau$ transformation extracts the result at h=0 rather than t=0.

A modification of Stolt's f-k algorithm derives this transformation. The single square root equation for downward continuation is

$$P(k_h,\omega,\tau) = P(k_h,\omega,\tau{=}0)\ e^{-i\Omega\tau} \qquad (1)$$

where $z = v\tau$ and Ω is the frequency domain conjugate of τ. The non-retarded dispersion relation is

$$\Omega = \left[\omega^2 - v^2 k_h^2\right]^{1/2} \qquad (2a)$$

To reduce f-k wrap-around problems the retarded dispersion relation is used.

$$\Omega = \omega - \left[\omega^2 - v^2 k_h^2\right]^{1/2} \tag{2b}$$

Extrapolated events line up near the diagonal $t=\tau$. Stolt's technique is used to derive the transformation formula:

(1) Write out equation 1 as a Fourier transform in (h,t) coordinates.

(2) Substitute Ω coordinates for ω using equation 2b.

(3) Apply the the imaging condition $h=0$.

(4) What remains is an inverse Fourier transform in $t-\tau$ coordinates.

$$P(\tau,t) = \int_{-\infty}^{\infty} \int_{-\infty}^{\infty} d\Omega d\omega e^{i\Omega\tau} e^{-i\omega t} \; P(k_h \to \Omega,\omega) \frac{dk_h}{d\Omega} \tag{3}$$

Solving for $P(h,t)$ in equation 1 instead of $P(t,\tau)$ in the same manner leads to the inverse transformation

$$P(h,t) = \int_{-\infty}^{\infty} \int_{-\infty}^{\infty} d\Omega dk_h e^{-ik_h h} e^{i\omega t} \; P(\Omega \to k_h,\omega) \frac{d\Omega}{dk_h} \tag{4}$$

Thus, according to equations 3 and 4, the $t-\tau$ transformations are accomplished by resampling and rescaling the data in the 2-D frequency domain.

There are a number of practical considerations in implementing equations 3 and 4:

(1) The parameter v is called the transformation velocity. The closer v is to the actual velocity, the tighter events will focus in $t-\tau$ space. However, since evanescent energy is thrown away in a Stolt mapping, v should be the lowest velocity present on the gather, which is usually water velocity.

(2) The overall data manipulations are the same for each transformation so that the same program can be used for either equation. The only difference is that the forward transform uses equation 2b to compute Ω as a function of k_h and vice-versa for the inverse transform.

(3) Because the frequency domain mapping (equation 2b) is non-linear, lots of zeroes should be padded along the h or τ axis to avoid problems.

(4) There is no harm done dropping the wave number ratios at the end of equations 3 and 4.

Enhancing Focii in Time-Depth Space

The second stage of the data restoration framework is to make events in model space look like they would have appeared had the data been better sampled. Figures 2, 5, and 9 are time-depth plots of a synthetic and two real data gathers in figures 1, 4, and 8. All of the source gathers have coinciding multi-velocity events, the real data cases being primaries and multiples. The transformation velocity in each case was near the lowest event velocity. Therefore, the low velocity events focus near the diagonal $t=\tau$, while higher velocity events focus less well at $\tau>t$. The goal is to enhance the focii throughout model space. After dozens of experiments, the following strategies seem to work best:

(1) Model space is *windowed* to remove f-k wrap-around and offset truncation effects. Regions $\tau<t$ and $\tau>t*maxv/v$ are zeroed.

(2) The focii are *sharpened* by a signed power of 1.3 .

(3) A *shaping weight* is applied in one of two ways.

(a) The ratio of the power of 75% over 100% of the existing offsets.

(b) An approximation of (a) which is a radially increasing weight of $1.+2.*\alpha$, where *alaha* is the angle in radians from the $t=\tau$ diagonal.

It is by no mean certain that there are not better strategies.

Examples I

Figures 1 through 11 are a synthetic and two real data examples of this extrapolation method. Each example shows the source gather, model space, and extrapolated gather. There is one example of the enhanced model space (figure 10). Also there is one example of the forward-reverse transform (figure 6) to demonstrate that it works.

The synthetic example worked rather well. The real data examples did not extend energy as far out. It is clear in all of the examples that all of the velocities are being extended. For the real data examples, I have found ways to strongly extend one of the velocities at the expense of the other velocity events. It is in balancing the multiple velocities that the ability to make long extensions is limited. However, I am optimistic that further experiments can improve these abilities.

Offset-Squared Time-Squared Transform

The mathematics of this transformation are so simple that only implementation details need be discussed. Being a non-linear transform, either the near offsets and low times are under-sampled or the wide offsets and late times oversampled (see figure 15). It was a surprise to the author that only a four-fold increase in squared space traces gave near perfect inverse transforms. A workable solution is to tune the transformation separately for near and wide offsets. Only a couple dozen model space traces are necessary for the auto-regressive portion of the extrapolation.

Extending Line Segments in Squared Space

The auto-regressive prediction algorithm for extrapolating data (invented by Rob Clayton) has been written up elsewhere (Thorson, this SEP volume). Tunable parameters are the number of source traces used (10 to 15) and the length of the prediction filter (1/3 to 2/5 the number of source traces). These factors are somewhat data dependent.

A problem with auto-regressive extrapolation used this way is the globality introduced by time Fourier transform. Often the algorithm tends to latch onto the strongest energy dip and extrapolate weaker events at this wrong dip. Decomposing the dataset into 1 sec time windows overlapping every .5 second reduces these global effects.

Examples II

Figures 12 through 16 include a synthetic and real data example using this method. Each example includes the source gather, model space, and and extrapolated result. As before, the synthetic example worked better, but both examples extrapolate multi-velocity events.

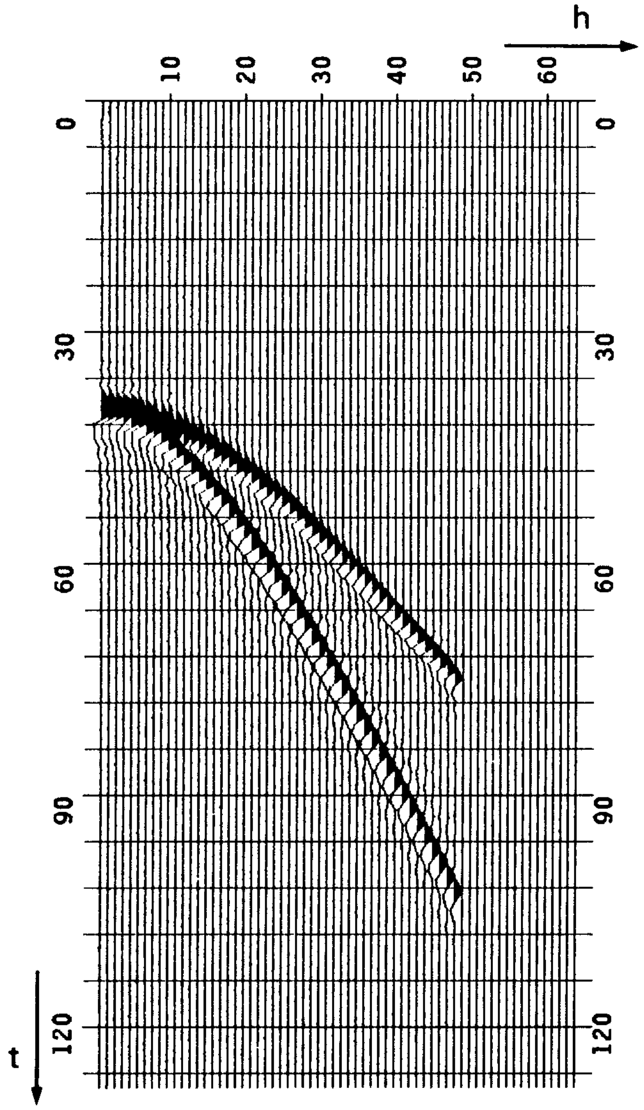

FIG. 1. Source synthetic gather for time-depth extrapolation. Generated by a Stolt constant velocity modelling program. Parameters are: nt=128 nx=48 dt=1. dx=1. v=1. and 1.5 tevent=33.

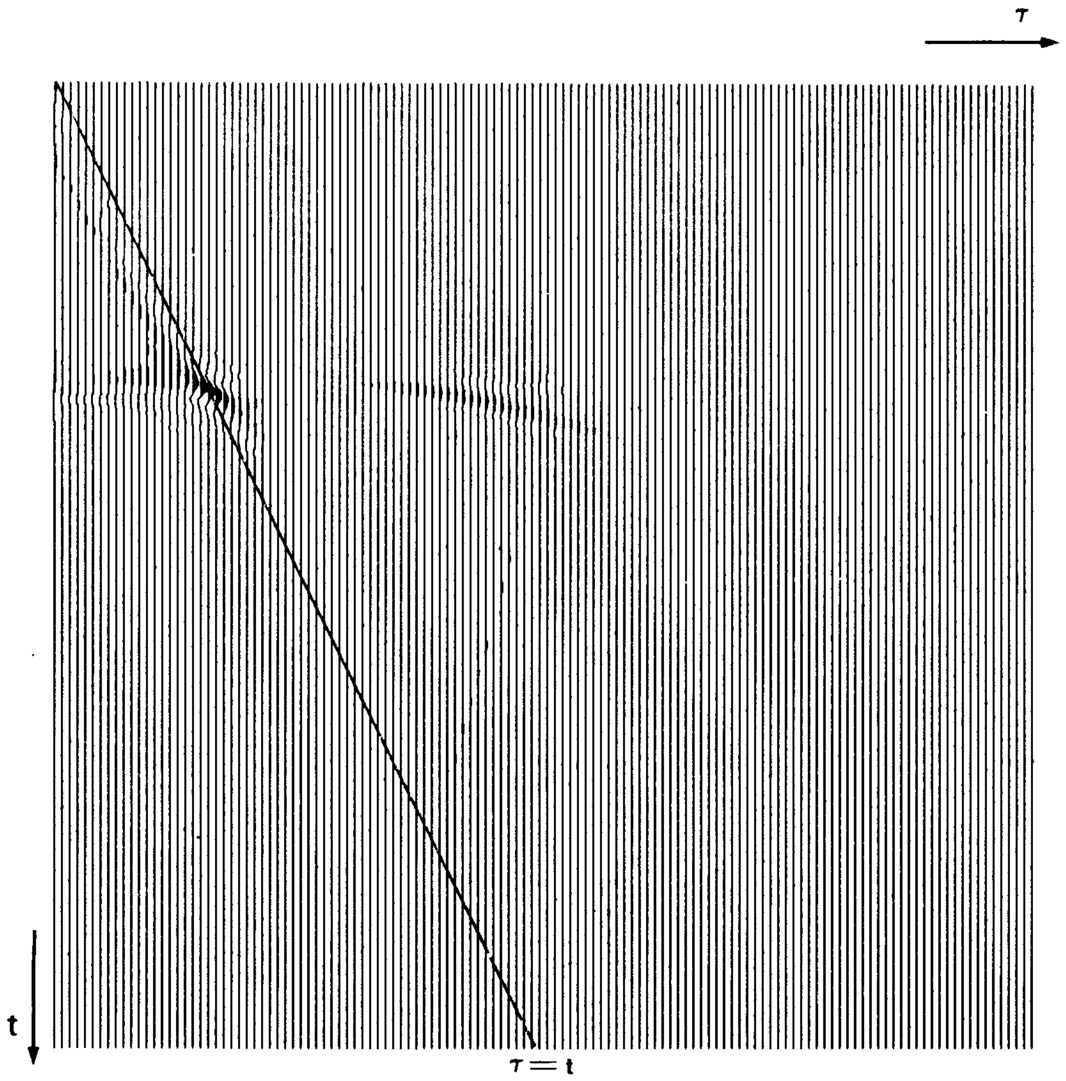

FIG. 2. Time-depth transformation of gather from figure 1. Transformation velocity was v=1. The low velocity event focuses fairly sharply along the $\tau = t$ diagonal. The high velocity event focuses less well at $\tau > t$. Other streaks are truncation and f-k wrap-around artifacts. Parameters are: nt=128 nτ=1.6 dt=1. dτ=2. v=1.
Because of the good separability of coinciding multi-velocity events, time-depth space is also an excellent domain for velocity filtering.

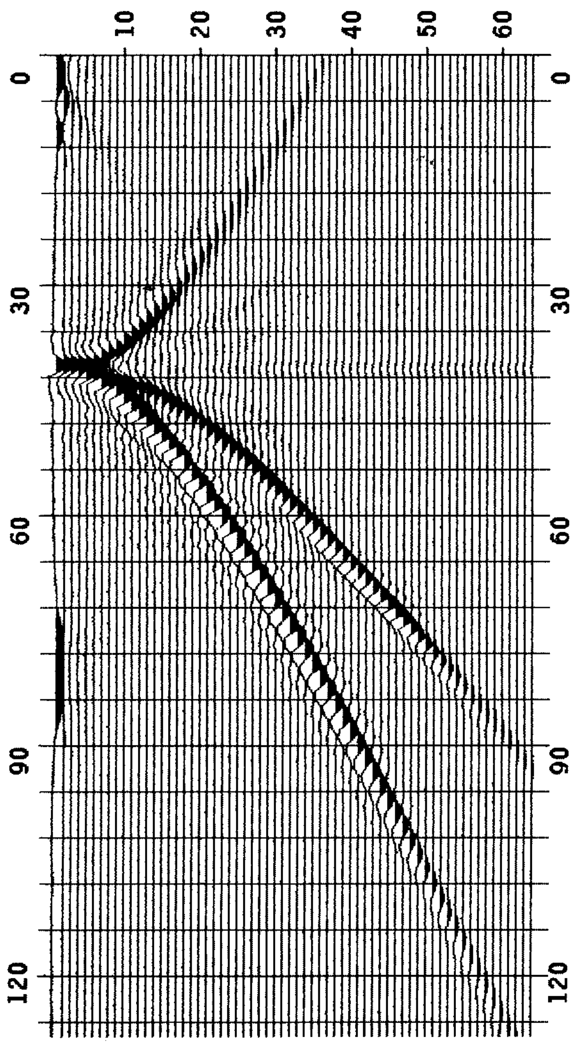

FIG. 3. Time-depth extrapolation off wide offsets of gather from figure 1. The extrapolation went rather well for both velocity events. The time-depth space focii in figure 2 were modified by a radially increasing weight and raised to the 1.3 power. The up-bowing artifact is due to enhancement of enegy in the region $\tau<t$. The remedy to window time-depth space as described in the text.

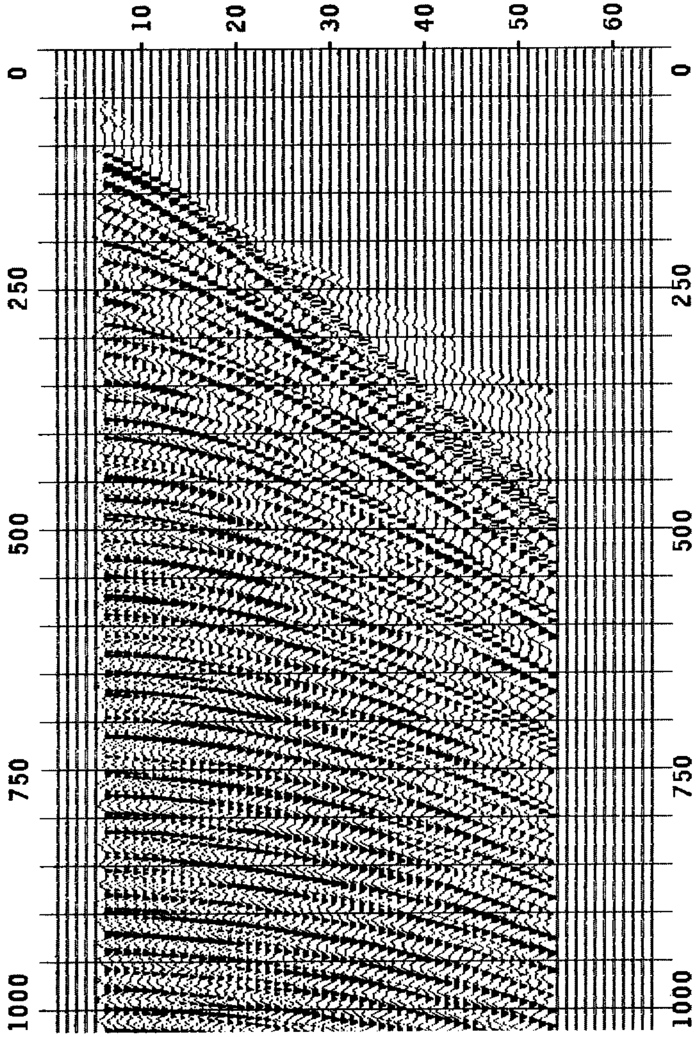

FIG. 4. Real data gather supplied by Amoco from offshore east Canada. Contains both primaries and water bottom multiples. (View side on to see multiples.) Parameters are: nt=1024 nx=48 dt=.004 x1=.273 dx=.05

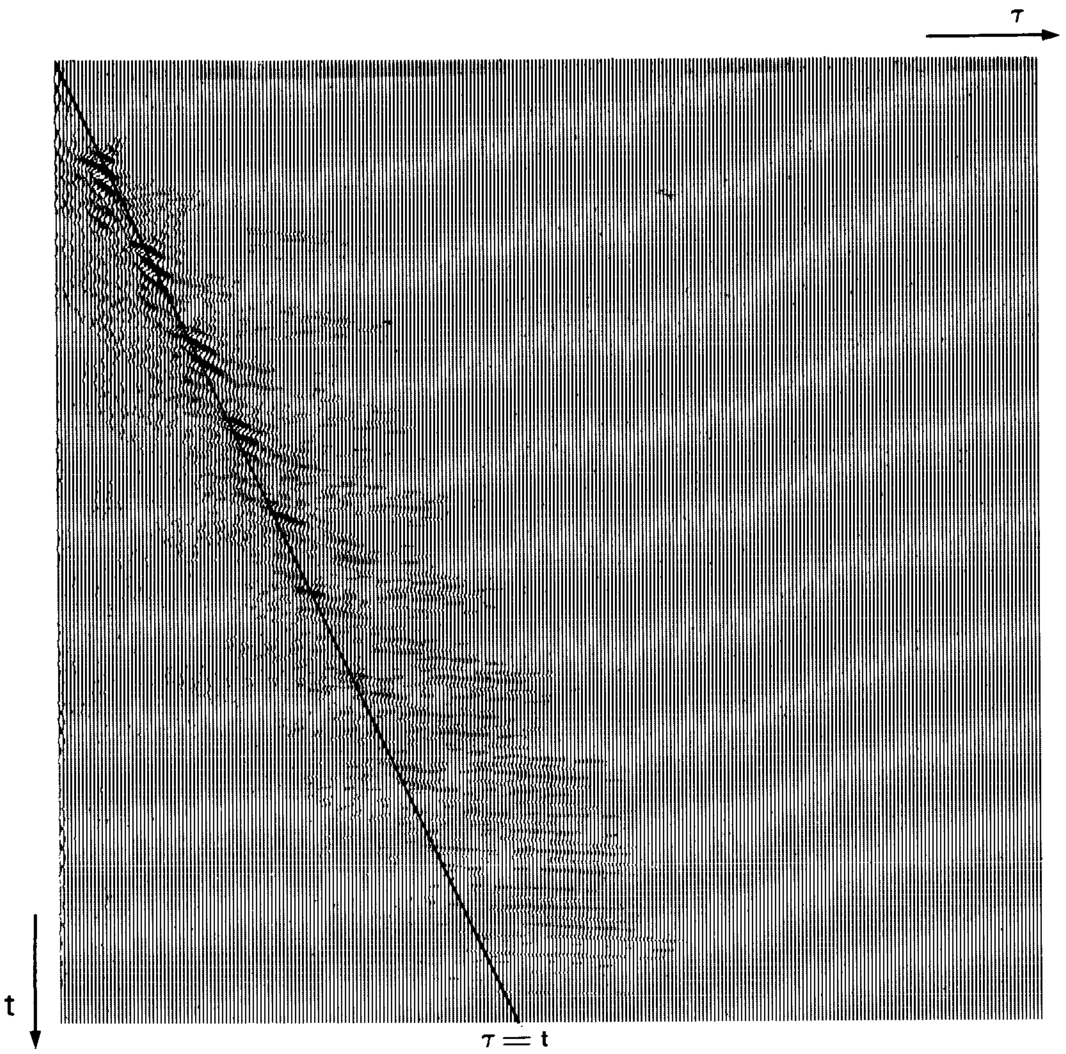

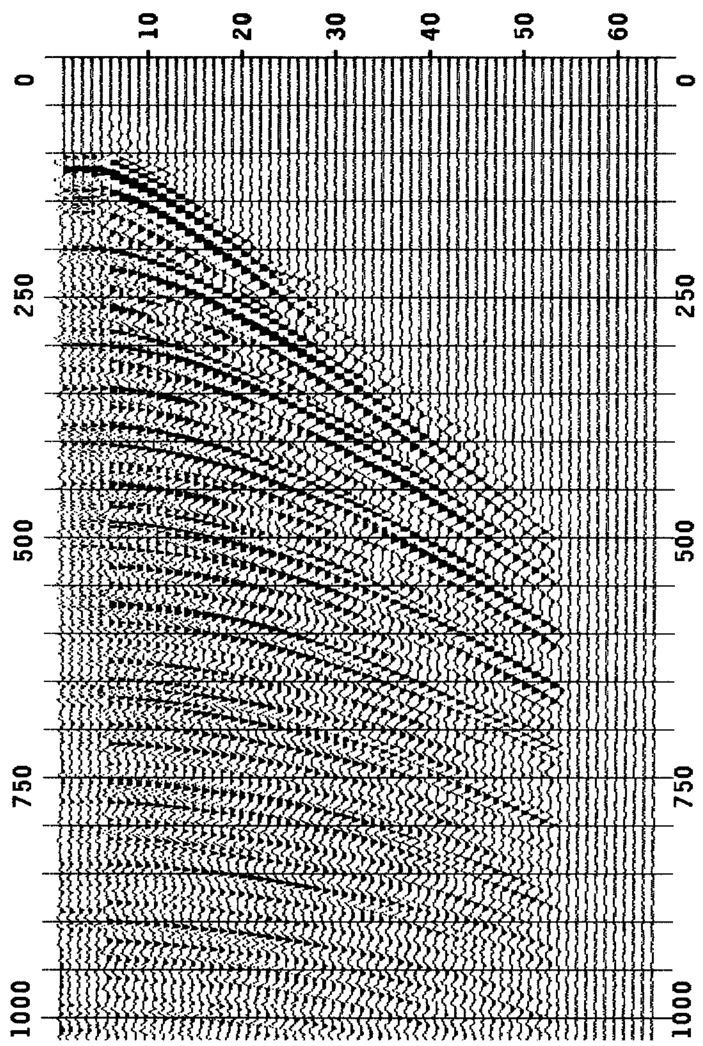

FIG. 5. Time-depth transform of gather from figure 4. Multiples are strongly focused to the left. Primaries focus less well to the right of multiple focii. There are a few f-k wrap-around and truncation artifacts in the region $\tau<t$. Parameters are: nt=1024 nτ=256 dt=.004 dτ=.05 v=1.45

FIG. 6. Inverse time-depth transform of data from figure 5. Because no modifications were made to the data in time-depth space, this figure should be identical to figure 4. This is the case, except for the near offsets which should be zero. These caused by numerical bugs in the program.

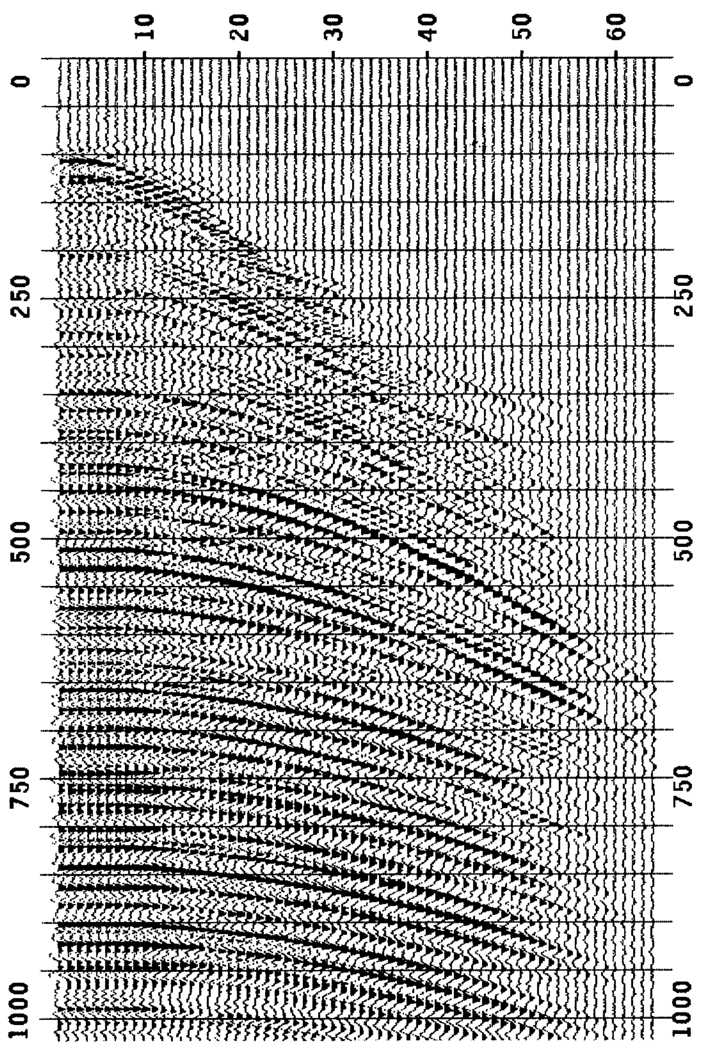

FIG. 7. Time-depth extrapolation of gather from figure 4. Time-depth space focii were enhanced by windowing, a 1.3 power sharpening, and smoothed shaping weight computed from the first 36 offsets. Both primaries and multiples are extended, though not as strongly as in the synthetic example. There are a few up-bowing arc artifacts due to imperfect windowing in time-depth space.

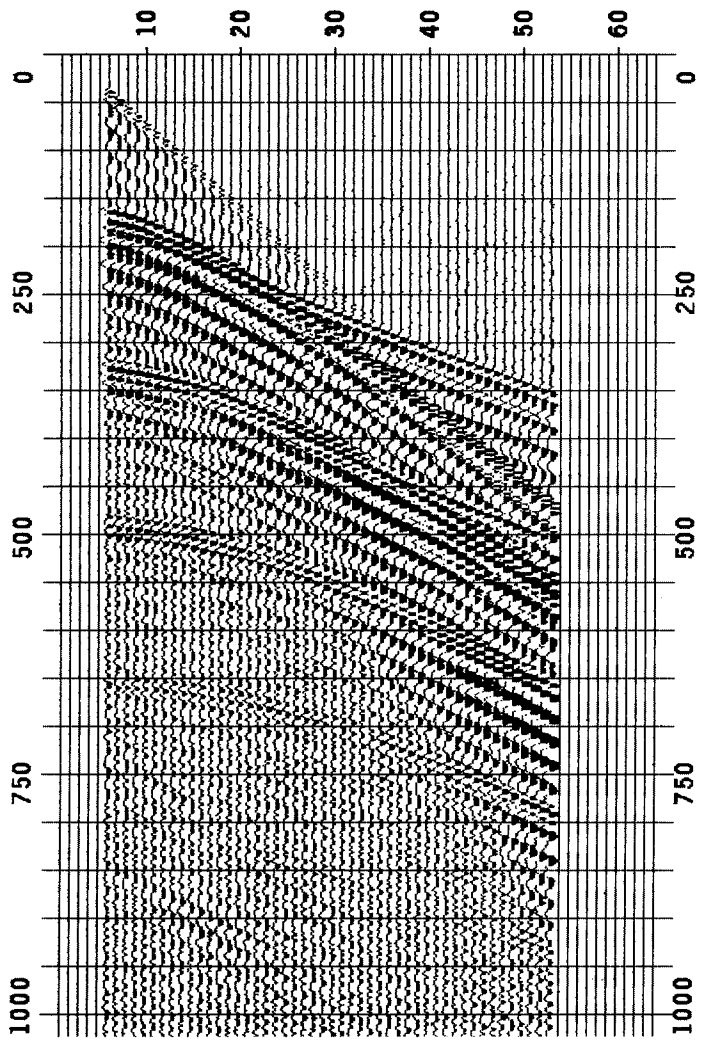

FIG. 8. Source gather for second real data extrapolation example. This data was supplied by GECO from offshore Norway and used by Thorson and Morley elsewhere in this SEP volume. Parameters are: nt=1024 nx=48 dt=.004 x1=.256 dx=.05

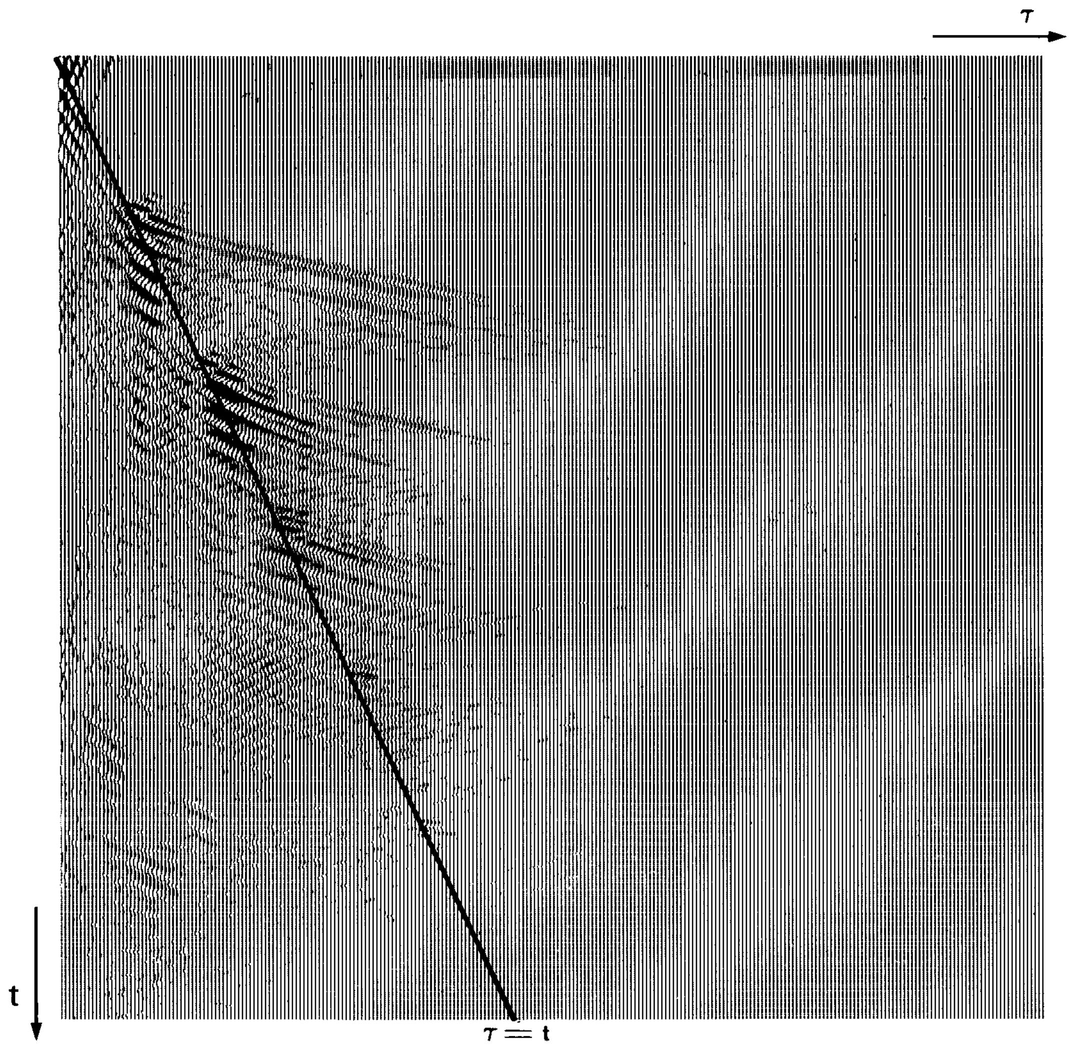

FIG. 9. Time-depth transformation of gather from figure 8. There are a few f-k wrap-around and truncation artifacts in the region $\tau < t$. Parameters are: nt=1024 nτ=256 dt=.004 dτ=.05 v=1.45

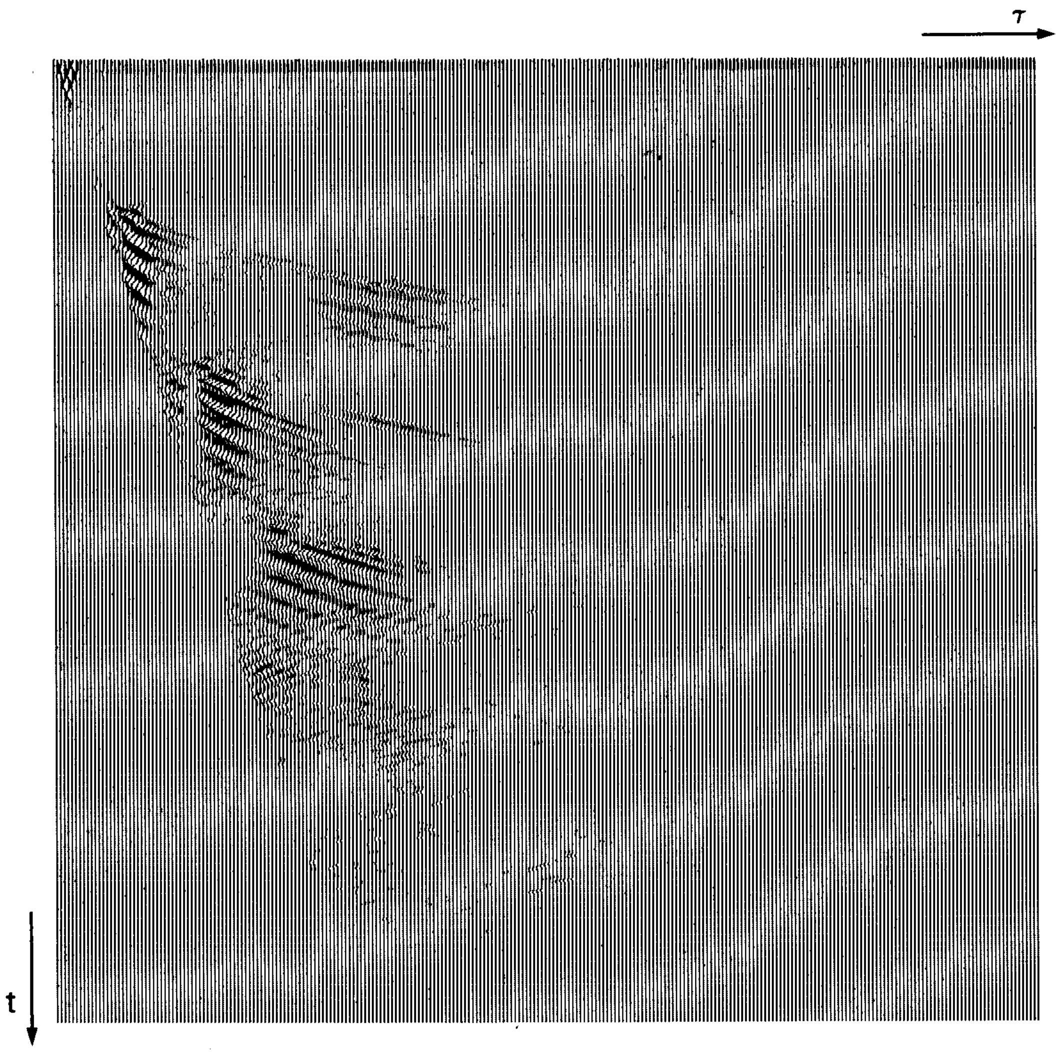

FIG. 10. Enhanced focii in time-depth space. Compare to figure 9. Time-depth space focii were enhanced by windowing, a 1.3 power sharpening, and smoothed shaping weight computed from the first 36 offsets.

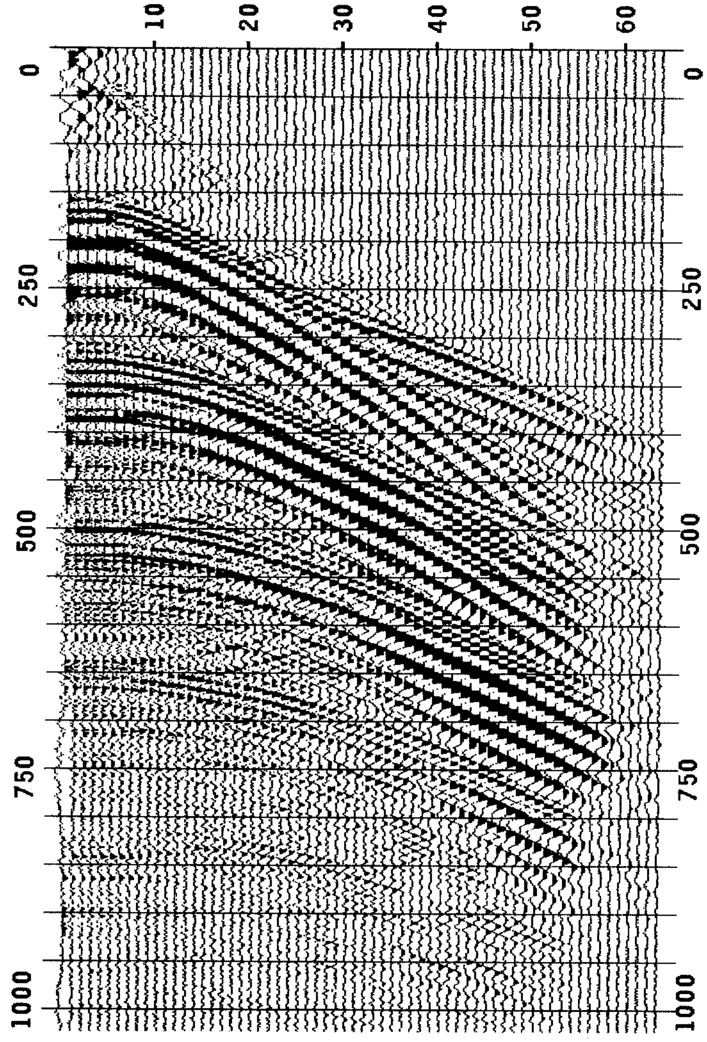

FIG. 11. Time-depth extrapolation of gather from figure 8. Time-depth space focii were enhanced by windowing, a 1.3 power sharpening, and smoothed shaping weight computed from the first 36 offsets. Both primaries and multiples are extended, though not as strongly and in the synthetic example. There are a few up-bowing arc artifacts due to imperfect windowing in time-depth space.

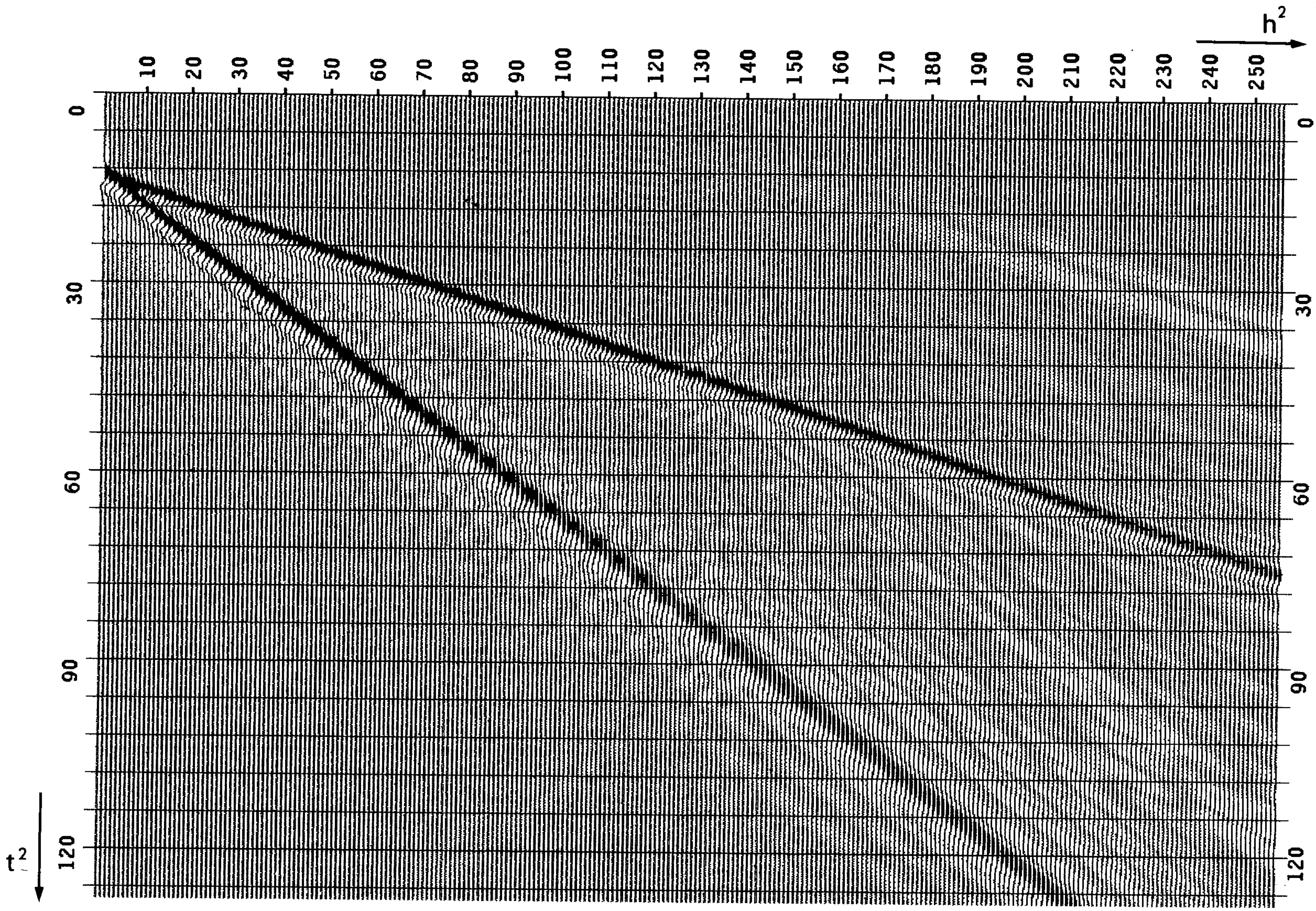

FIG. 12. Offset-squared time-squared transform of synthetic gather from figure 1. Traces 1 - 128 are from the original data. Hyperbolic events map into straight lines. Events of different velocities have different slopes. Parameters are: nt=128 nx=256 dt=17.39 dx=17.39

Traces 129 - 256 have been extrapolated from the original data using auto-regressive prediction as described in the text. A 32 coefficient filter was computed from 128 source traces. The events are extrapolated rather well, though thee is a slight loss in energy at the widest offsets. There is a little noise in the extrapolated region, probably due to numerical problems.

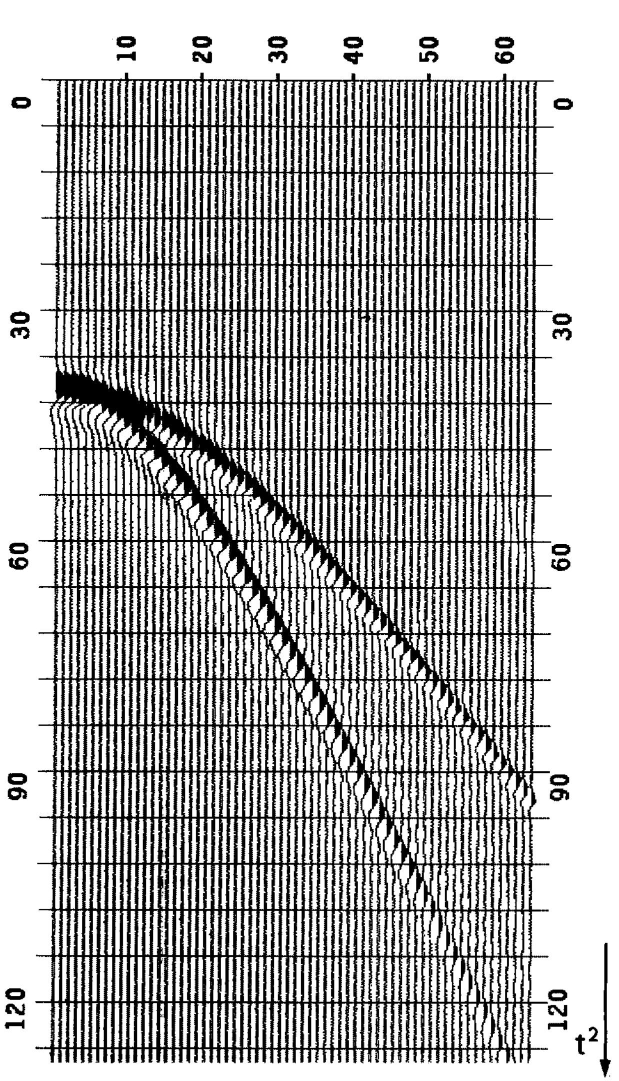

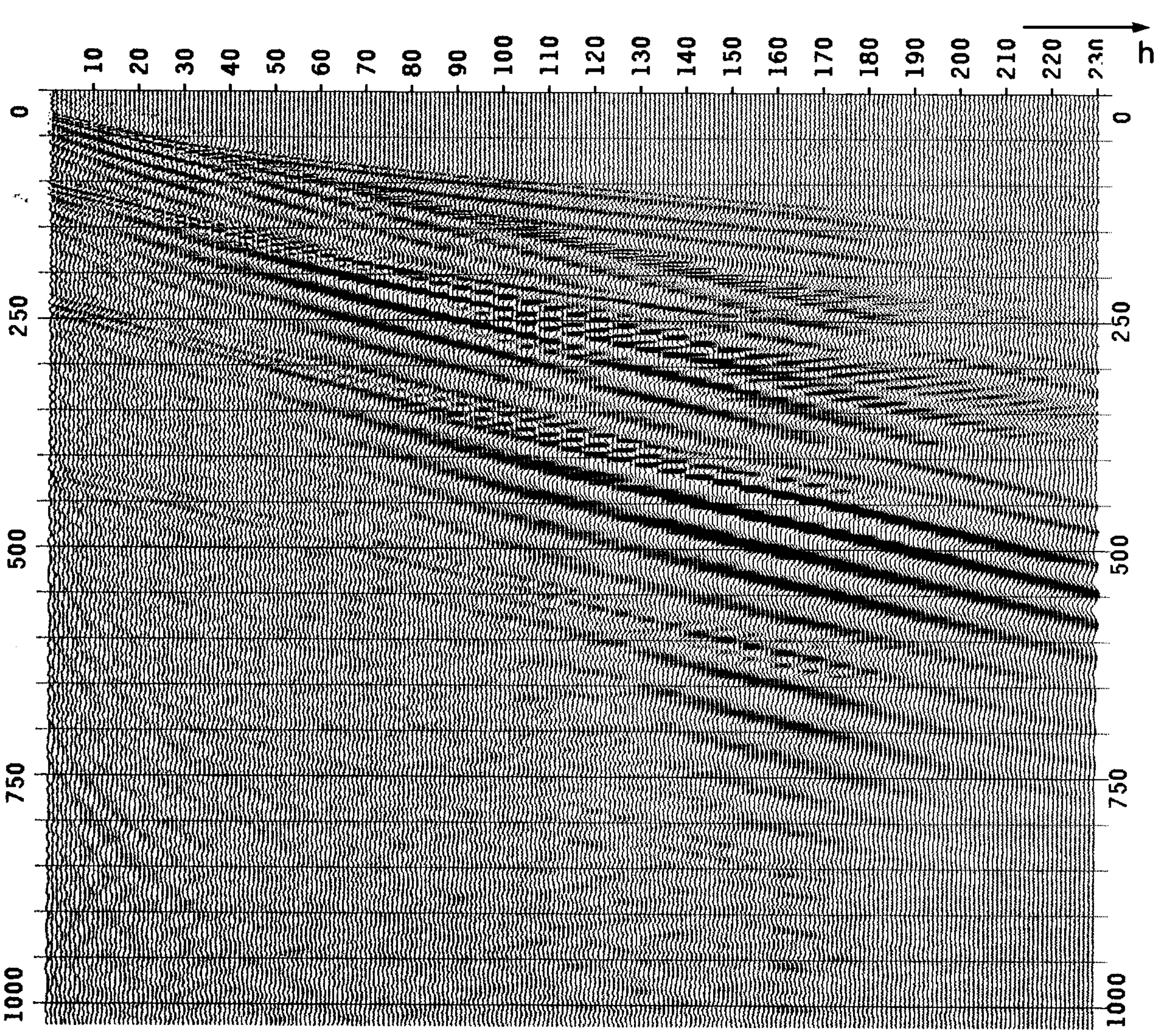

FIG. 13. Extrapolation of wide offsets off of synthetic gather from figure 1 using the offset-squared time-squared method. The quality of extrapolation is excellent. There is a minor artifact near time 60 as explained in the previous figure.

FIG. 14. Offset-squared time-squared transform and extrapolation of the real data gather from figure 8. Traces 1-160 are from the original data. Hyperbolic events map into straight lines. Events of different velocities have different slopes. The non-hyperbolic noise in the lower left of figure 7 map into curve lines in the lower left of this figure. Because the transformation mapping was done along the direction of the coordinate axes, there is some dip aliasing at wide offsets. Parameters are: nt=1024 nx=230 dt=.016 x1=.066 dx=.041
Traces 160 - 230 have been extrapolated from the traces 130 - 160 using a 11 coefficient auto-regressive prediction filter. The prediction was performed on 1 sec windows overlapping every .5 sec to avoid the globality and wrap-around effects of the Fourier transform. The stronger events extrapolate somewhat better than the weaker ones. It is surprising to see how well the character of the aliased events extrapolates.

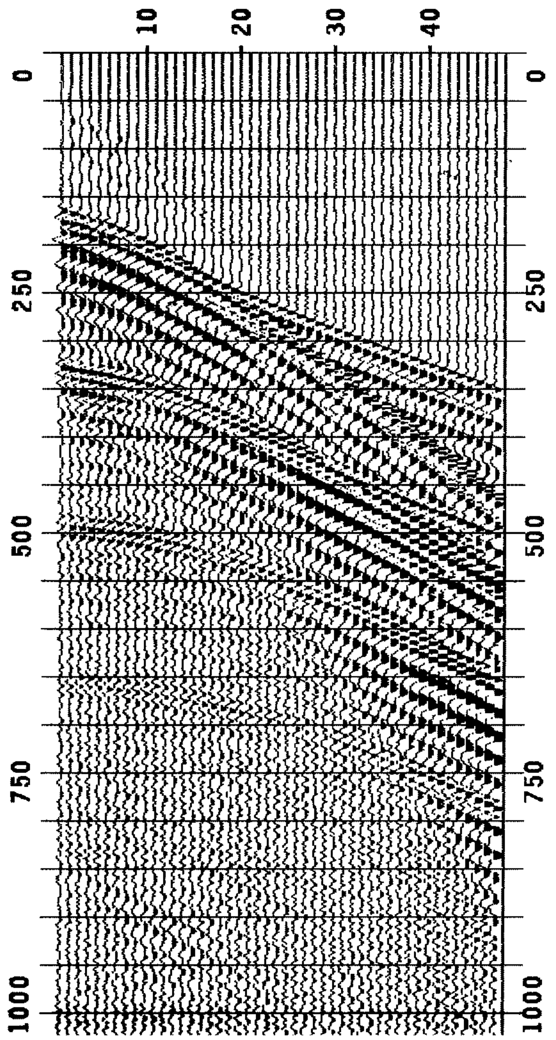

FIG. 15. Inverse transform of the original data from figure 14 to demonstrate the fidelity of the forward-reverse mapping. Compare this figure to the original in figure 8. There is some loss in the upper left corner where the mapping was undersampled, but otherwise the fidelity was surprisingly good.

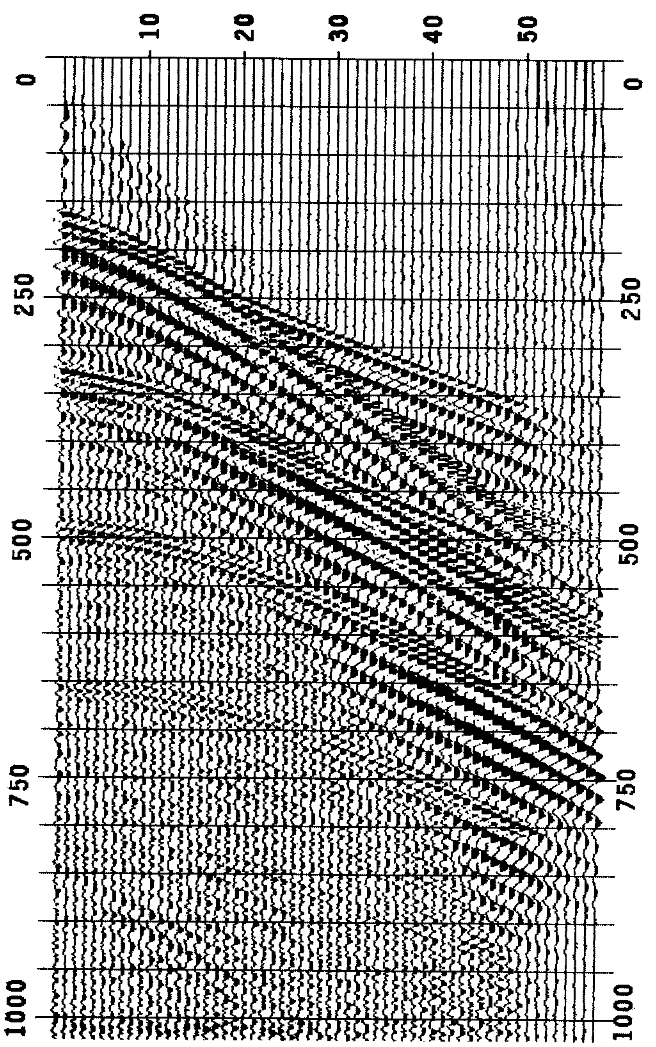

FIG. 16. Offset-squared time-squared extrapolation of wide offsets off of the gather from figure 8 (.i.e. the inverse transform of all of the traces from figure 14). Both multiples and primaries are extrapolated, though the result is not as good as the synthetic. A little more care need be taken in tuning the auto-regressive prediction parameters. Wide offset, low time artifacts are frequency domain wrap-around artifacts.